Journal of Medicinal Chemistry

BRIEF ARTICLE

pubs.acs.org/jmc

Toluidinesulfonamide Hypoxia-Induced Factor 1 Inhibitors: Alleviating Drug−Drug Interactions through Use of PubChem Data and Comparative Molecular Field Analysis Guided Synthesis

Bernd Wendt,* Marcel Mülbaier, Sabine Wawro, Christoph Schultes,† Jorge Alonso, Bernd Janssen, and Joe Lewis

Elara Pharmaceuticals GmbH, Boxbergring 107, 69127 Heidelberg, Germany

Supporting Information

ABSTRACT: Inhibitors of hypoxia-inducible factor 1 (HIF-1) represent promising anticancer therapeutics. We have identified a series of potent toluidinesulfonamide HIF-1 inhibitors. However, the series was threatened by a potential liability to inhibit CYP2C9 which could cause dangerous drug−drug interactions when being coadministered with other drugs. We used structure−activity data from the PubChem database to develop a topomer CoMFA model that guided the design of novel sulfonamides with high selectivity for HIF-1 over CYP2C9 inhibition.

INTRODUCTION

Hypoxia-inducible factor-1 (HIF-1) is a transcription factor that promotes in response to hypoxic conditions the production and release of growth factors required for the development of new blood vessels, e.g., vascular endothelial growth factor (VEGF), proteins controlling glucose metabolism, and other mediators.[1] Hypoxia is a common feature in solid tumors, as existing blood vessels cannot supply the rapidly growing tumor with sufficient oxygen and nutrients.[2] The HIF signaling pathway therefore is crucial for the growth of tumors, and overexpression of HIF is often associated with an advanced disease stage and poor survival prognosis of cancer patients.[3]

Because of the importance of HIF-1 in tumor development, progression, and metastasis, a considerable amount of effort has been devoted to identify HIF-1 inhibitors for cancer therapy.[4−7] However, these compounds often have activities other than HIF-1 inhibition, and most of them lack the desired pharmacokinetic properties or toxicity profiles required for a useful pharmaceutical agent. Furthermore, some of the compounds have the disadvantage that they cannot be administered orally, such as the HIF-1 inhibitor EZN-2968, which is a locked nucleic acid antisense oligonucleotide.[8]

Our lead **1** is a potent inhibitor of hypoxia-induced HIF-1 activation as measured by a cell-based reporter assay (Invitrogen). Compound **1** also has a strong inhibitory effect on cell proliferation in a panel of human cancer cell lines such as MCF7, HCT-116, and MIAPaCa. According to literature precedence, arylsulfonamides have been characterized as CYP2C9 inhibitors;[9] hence, we assumed that our lead compound also had a potential liability as inhibitor for this enzyme. Therefore, we explored the structural requirements for CYP2C9 inhibition, hoping to find divergent SAR between CYP2C9 and HIF-1 inhibition.

CYP2C9 is a major cytochrome P450 enzyme involved in the metabolic clearance of a wide variety of therapeutic agents. Dangerous drug−drug interactions can arise when a CYP2C9 inhibitor is administered together with drugs possessing a low therapeutic index.[10] Patients may face life-threatening situations as a result of the diminished CYP2C9 enzyme activity and a higher than expected exposure to their prescribed standard drug.

In attempts to eliminate potential CYP2C9 inhibitors early in the drug discovery process, many computational models have been proposed for the interaction of drugs with CYP2C9.[11,12] In addition, three crystal structures of CYP2C9 are available.[13,14] Despite such valuable tools to generate structure−activity models, because of the inherent flexibility of the CYP2C9 protein's active site and its ligand promiscuity, considerable challenges remain for structure-based methods.[15,16] However, superior results could be achieved using ligand-based methods.[17] In general, three-dimensional quantitative structure−activity relationship (3D-QSAR) studies have been very successful in rationalizing many data sets of ligands and predicting their affinities to CYP2C9.[18−20] A prerequisite for good QSAR predictions is activity data on structurally similar ligands. We were fortunate to find a large number of ligands similar to our lead compound, where CYP2C9 data are reported in one of the largest public chemical biology databases.

RESULTS AND DISCUSSION

A substructure search in PubChem[21] using *N*-phenylbenzenesulfonamide as a query yielded 978 virtual hits with associated activity information from a CYP2C9 high-throughput screen. Initially, the HQSAR[22] (a 2D-QSAR method) was attempted to derive a global QSAR model on this data set using the percent inhibition values as dependent variable. This yielded moderate relationships with an ensemble leave-one-out cross-validated r^2 (LOO-q^2) of 0.3. Depending on the hologram length, the predicted value for our lead compound varied between 30% and 60% inhibition of CYP2C9 at 5 μM. Apart from the inconclusive result from HQSAR, these models did

Received: March 8, 2011
Published: May 16, 2011

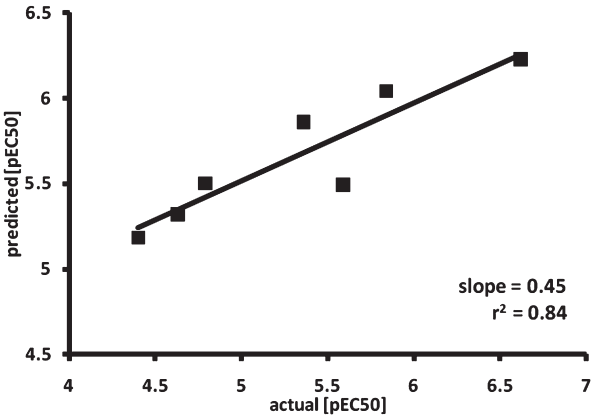

Figure 1. Actual pEC_{50} for CYP2C9 inhibition plotted against values predicted from the topomer CoMFA model.

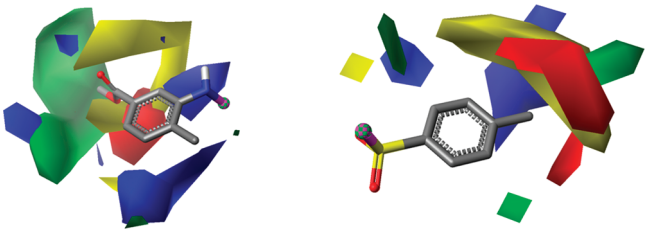

Figure 2. Topomer representation of **1**: amino fragment on the left and sulfonyl fragment on the right with contours from the topomer CoMFA model of CYP2C9 inhibition. Green and yellow contours highlight favored and disfavored steric interactions, whereas red and blue contours highlight favored negative and positive electrostatic interactions (disfavored positive and negative electrostatic interactions).

not allow for structural interpretation. Therefore, we explored the use of the quantitative series enrichment analysis (QSEA)[23] method for deriving local 3D-SAR from chemical biology data.[24] In QSEA, the ligands of the data set are organized around its centroid, and topomer CoMFA[25] models are being created, starting with the centroid compound and its two nearest neighbors and then iteratively expanding the training set one by one with the next similar compound, each time creating a new topomer CoMFA. The consecutive LOO-q^2 values for our data set reached a plateau between training set sizes of 115−127, indicating a robust SAR. We chose the topomer CoMFA model with a training set size of 122 and a q^2 of 0.21 as 3D-QSAR model for structural interpretation and prediction.[26] Good and predictive CoMFA models are suggested to have $q^2 > 0.3$[27] A low q^2 may simply reflect the lack of redundancy[28] in the data set; however, a high q^2 does not sufficiently indicate good predictivity.[29] Using systematic exploration of topomer CoMFA models with QSEA, where the aim is to navigate within the model space built from available structures and activities, we suggest setting the threshold of q^2 to >0.2 whenever an enrichment of significant q^2 is observed. Surprisingly, irrespective of the low q^2 derived from the training set, the model's predictions for seven newly synthesized compounds showed a rather low SDEP of 0.54 (see Figure 1). The overall correlation is good, indicating that the structural modifications proposed by the model turned out to be predicted in the right direction. However, the slope of the trend line is rather flat. It seems that the quality of the biological information

Table 1. Toluidinesulfonamides and Biological Activities for HIF-1 and CYP2C9 and Predicted Values from Topomer CoMFA Model

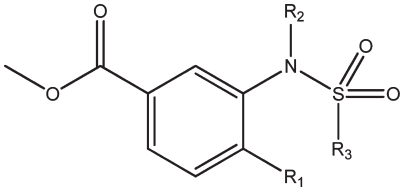

cmpd	R_1	R_2	R_3	pIC50 Hif-1	pEC50 CYP2C9 exp.	pred.
1	Me	H	4-Me-Ph	7.4	5.8	6.00
2	Me	H	4-MeO-Ph	7.2	5.4	5.90
3	Me	H	3,4-di-(MeO)-Ph	<5	5.6	5.50
4	Me	H	4-acetamido-Ph	4.7	6.6	6.20
5	MeO	H	4-MeO-Ph	5.5	4.4	5.20
6	Me	Me	4-Me-Ph	5.8	4.8	5.50
7	Me	Me	4-MeO-Ph	6.2	4.6	5.30
8	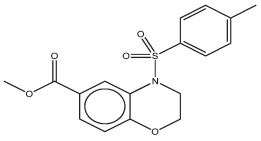			7	5.4	-

at hand was sufficient to detect the trend but proved to be inadequate to properly forecast its steepness.

The topomer CoMFA afforded a structural interpretation of the altered patterns in the ligands that lead to differences in CYP2C9 inhibition. The contour plots of the topomer CoMFA model are shown for analogues of **1** in Figure 2, in its topomer representation, as a pair of directly bonded amino and sulfonyl fragments. The amino fragment (Figure 2, left) shows major steric contributions to CYP2C9 activity in the 5- and 6-position and major electrostatic contributions in the 1- and 2-position of the aromatic ring. Whereas larger substitutions in position 5 (green contours) favor CYP2C9 inhibition, substituents in position 6 (yellow contours) disfavor CYP2C9 activity. Blue contours around the 1- and 2-position indicate favorable interactions for hydrocarbon substituents.

The contour plots of the sulfonyl fragment (Figure 2, right) revealed major steric and electrostatic interactions in the 4-position with minor steric interactions in the 3-position. The model also suggests that extended substituents are in favor of CYP2C9 inhibition (green contour) with heteroatoms favored in the farther part of the side chain (red contours) and electropositive hydrocarbons favored close to the aromatic ring (blue contours). All these suggestions from the model were further explored in the design of new analogues of our lead

dx.doi.org/10.1021/jm200272h |*J. Med. Chem.* 2011, 54, 3982–3986

Scheme 1. Synthetic Route to 1−7 in Table 1

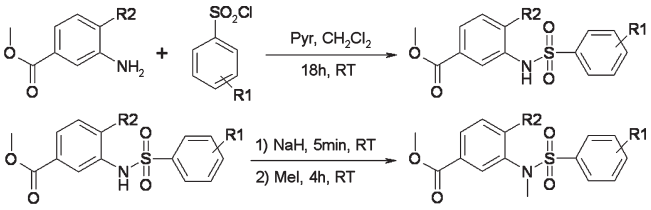

Scheme 2. Synthetic Route to 8 in Table 1

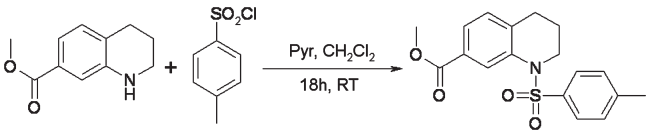

compound by introduction of new substituents at three positions (Table 1, Schemes 1 and 2).

Introduction of a methoxy group in the 4-position of the sulfonylphenyl fragment, as seen with **2**, shows a neutral effect on HIF-1 activity. However, as the topomer CoMFA suggests, this modification results in reduction of the CYP2C9 potency[30] with the electronegative oxygen pointing toward the blue contour, favoring electropositive interactions, and with the electropositive methyl hydrogens pointing toward the red contours, favoring electronegative interactions (Figure 3, right).

As seen with **3**, adding another methoxy substituent in the 3-position of the sulfonylphenyl fragment does not significantly reduce the off-target potency but interferes significantly with HIF-1 activity. The model also suggests that extended substitutions in the 4-position of the sulfonylphenyl fragment would lead to higher CYP2C9 potency, which is confirmed by **4** having an acetamido side chain in the 4-position and submicromolar activity reported for CYP2C9. With regard to the toluidine fragment, any modification of the 5-position in the toluidine ring had to be carefully judged because, based on established SAR, the ester group was crucial for maintaining HIF-1 activity. Here, the model suggests introducing a methoxy group to the 2-position of the toluidine ring, thereby exposing the electronegative oxygen next to a region where electropositive interactions are favored and filling up space where steric interactions are disfavored, as illustrated by **5** (Figure 3, left). This modification almost wipes out CYP2C9 potency; unfortunately this also goes along with a large drop in HIF-1 activity. A further suggestion from the model is to substitute the sulfonamide nitrogen with small hydrocarbons like methyl. This results in a large reduction of CYP2C9 potency, as evidenced by **6**. Combining the effects of a methoxy substituent in the 4-position of the sulfonylphenyl fragment with alkylation of the sulfonamide nitrogen, as shown in **7**, is a promising strategy, since the drop in CYP2C9 potency comes with a lower impact on HIF-1 activity. Further combination of the effects of a methoxy-substituted toluidine ring and the methylated sulfonamide nitrogen eventually led to the discovery of a new scaffold. The benzoxazine sulfonamide **8** shows a promising selectivity window with a high preference for HIF-1 over CYP2C9 inhibition.

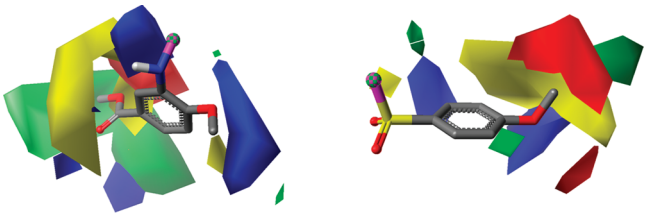

Figure 3. Topomer representation of **5**: amino fragment on the left and sulfonyl fragment on the right with contours from the topomer CoMFA model of CYP2C9 inhibition.

CONCLUSION

The 3D-QSAR model enabled the HIF-1 program to identify structural patterns of the ligands that cause unwanted CYP2C9 inhibition. Careful interpretation of the contours allowed us to design small changes within the toluidinesulfonamide series, yielding potent HIF-1 inhibitors with high selectivity over inhibition of CYP2C9. Combining the additive differences from these studies resulted in the discovery of a new potent benzoxazine series. Understanding potential CYP2C9 liabilities and designing compounds that are less likely to act as inhibitors are mandatory for a discovery project, especially at an early stage. The utilization of publicly accessible SAR data through a topomer CoMFA model is a suitable approach in this effort.

EXPERIMENTAL SECTION

All reactions involving air or moisture sensitive reagents were performed under nitrogen atmosphere using standard Schlenk techniques. Unless otherwise stated, chemicals and solvents were of reagent grade and used as obtained from commercial sources without further purification. Water was deionized. The reactions were monitored by thin-layer chromatography (TLC) analysis using silica gel (Merck 60-F254) plates. Compounds were visualized by UV irradiation and/or spraying with literature known stains followed by charring at 150 °C (Seebach stain: 2.5 g of molybdatophosphoric acid, 1.0 g of Ce(IV) sulfate, 6 mL of concentrated sulfuric acid, and 94 mL of water).

General Procedure for the Preparation of Sulfonamides. In a typical procedure, a flask was charged with 8 mL of methylene chloride. Then 165 mg (1.0 mmol) of methyl 3-amino-4-methylbenzoate, 1.0 equiv of the corresponding aromatic sulfonic acid, and 0.4 mL of pyridine were added. The flask was flushed with nitrogen, and the mixture was stirred overnight at room temperature. After completion, the reaction was quenched by addition of 10 mL of aqueous $KHSO_4$ solution (5% w/w) followed by extraction with ethyl acetate (3 × 10 mL). The combined organic layers were dried with Na_2SO_4, and the solvent was evaporated. The crude reaction product was further purified by preparative LCMS to afford the final products. Compound **8** was synthesized in an analogous procedure starting from commercially available methyl 3,4-dihydro-2*H*-benzo[*b*][1,4]oxazine-6-carboxylate. Compound **5** was synthesized in an analogous procedure starting from commercially available methyl 3-amino-4-methoxybenzoate.

General Procedure for the Preparation of N-Methylated Sulfonamides. In a typical procedure, 100 mg (1 equiv) of the corresponding sulfonamide was dissolved in 5 mL of dry THF. Sodium hydride (1.1 equiv) was added, and the mixture was stirred at room temperature until evolution of hydrogen has stopped (5 min). Then methyl iodide (1.1 equiv) was added and the mixture was further stirred for 4 h at room temperature. After completion, the reaction was quenched by addition of 20 mL of aqueous $KHSO_4$ solution (5% w/w) followed by extraction with ethyl acetate (3 × 10 mL). The combined organic layers were dried with Na_2SO_4, and the solvent was evaporated. The crude

reaction product was further purified by preparative LCMS to afford the final products.

■ ASSOCIATED CONTENT

Supporting Information. Spectroscopic data for **1**−**8**, assay protocols, dose-response curves, modeling parameters, and SAR table from PubChem including statistical information from QSEA. This material is available free of charge via the Internet at http://pubs.acs.org.

■ AUTHOR INFORMATION

Corresponding Author

*Phone: +49 6221 387 8850. Fax: +49 6221 387 8971. E-mail: b.wendt@elarapharma.com.

Present Addresses

[†]Merck-Serono GmbH, Alsfelder Strasse 17, 64289 Darmstadt, Germany.

■ ACKNOWLEDGMENT

This study is supported by the BMBF (Grant No. 0315418).

■ ABBREVIATIONS USED

3D, three-dimensional; CoMFA, comparative molecular field analysis; CYP2C9, cytochrome P450 2C9; EC_{50}, concentration of drug that produces a half-maximal response; HIF-1, hypoxia-inducible factor 1; HQSAR, hologram quantitative structure−activity relationship; IC_{50}, concentration of drug that produces a half-maximal inhibition; LOO, leave-one-out; QSAR, quantitative structure−activity relationship; QSEA, quantitative series enrichment analysis; SDEP, standard deviation of prediction error

■ REFERENCES

(1) Semenza, G. L. HIF-1 and tumor progression: pathophysiology and therapeutics. *Trends Mol. Med.* **2002**, *8*, S62–S67.

(2) Vaupel, P.; Mayer, A. Hypoxia in cancer: significance and impact on clinical outcome. *Cancer Metastasis Rev.* **2007**, *26*, 225–339.

(3) Semenza, G. L. Evaluation of HIF-1 inhibitors as anticancer agents. *Drug Discovery Today* **2007**, *12*, 853–859.

(4) Rapisarda, A.; Uranchimeg, B.; Scudiero, D. A.; Selby, M.; Sausville, E. A.; Shoemaker, R. H.; Melillo, G. Identification of small molecule inhibitors of hypoxia-inducible factor 1 transcriptional activation pathway. *Cancer Res.* **2002**, *62*, 4316–4324.

(5) Kung, A. L.; Zabludoff, S. D.; France, D. S.; Freedman, S. J.; Tanner, E. A.; Vieira, A.; Cornell-Kennon, S.; Lee, J.; Wang, B.; Wang, J.; Memmert, K.; Naegeli, H. U.; Petersen, F.; Eck, M. J.; Bair, K. W.; Wood, A. W.; Livingston, D. M. Small molecule blockade of transcriptional coactivation of the hypoxia-inducible factor pathway. *Cancer Cell* **2004**, *6*, 33–43.

(6) Welsh, S.; Williams, R.; Kirkpatrick, L.; Paine-Murrieta, G.; Powis, G. Antitumor activity and pharmacodynamic properties of PX-478, an inhibitor of hypoxia-inducible factor-1alpha. *Mol. Cancer Ther.* **2004**, *3*, 233–244.

(7) Chau, N. M.; Rogers, P.; Aherne, W.; Carroll, V.; Collins, I.; McDonald, E.; Workman, P.; Ashcroft, M. Identification of novel small molecule inhibitors of hypoxia-inducible factor-1 that differentially block hypoxia-inducible factor-1 activity and hypoxia-inducible factor-1alpha induction in response to hypoxic stress and growth factors. *Cancer Res.* **2005**, *65*, 4918–4928.

(8) Greenberger, L. M.; Horak, I. D.; Filpula, D.; Sapra, P.; Westergaard, M.; Frydenlund, H. F.; Albaek, C.; Schrøder, H; Ørum, H. A RNA antagonist of hypoxia-inducible factor-1alpha, EZN-2968, inhibits tumor cell growth. *Mol. Cancer Ther.* **2008**, *7*, 3598–3608.

(9) Miners, J. O.; Birkett, D. J. Cytochrome P4502C9: an enzyme of major importance in human drug metabolism. *Br. J. Clin. Pharmacol.* **1998**, *45*, 525–538.

(10) Rettie, A. E.; Jones, J. P. Clinical and toxicological relevance of CYP2C9: drug−drug interactions and pharmacogenetics. *Annu. Rev. Pharmacol. Toxicol.* **2005**, *45*, 477–494.

(11) Payne, V. A.; Chang, Y. T.; Loew, G. H. Homology modeling and substrate binding study of human CYP2C9 enzyme. *Proteins* **1999**, *37*, 176–190.

(12) De Groot, M. J.; Alex, A. A.; Jones, B. C. Development of a combined protein and pharmacophore model for cytochrome P450 2C9. *J. Med. Chem.* **2002**, *45*, 1983–1993.

(13) Williams, P. A.; Cosme, J.; Ward, A.; Angove, H. C.; Matak-Vinkovic, D.; Jhoti, H. Crystal structure of human cytochrome P450 2C9 with bound warfarin. *Nature* **2003**, *424*, 464–468.

(14) Wester, M. R.; Yano, J. K.; Schoch, G. A.; Griffin, K. J.; Stout, C. D.; Johnson, E. F. Crystal structure of p4502c9 with flurbiprofen bound. *J. Biol. Chem.* **2004**, *279*, 35630–35637.

(15) Afzelius, L.; Zamora, I.; Masimirembwa, C. M.; Karlén, A.; Andersson, T. B.; Mecucci, S.; Baroni, M.; Cruciani, G. Conformer- and alignment-independent model for predicting structurally diverse competitive CYP2C9 inhibitors. *J. Med. Chem.* **2004**, *47*, 907–914.

(16) Sun, H.; Scott, D. O. Structure-based drug metabolism predictions for drug design. *Chem. Biol. Drug Des.* **2010**, *75*, 3–17.

(17) Sykes, M. J.; McKinnon, R. A.; Miners, J. O. Prediction of metabolism by cytochrome P450 2C9: alignment and docking studies of a validated database of substrates. *J. Med. Chem.* **2008**, *28*, 780–791.

(18) Jones, B. C.; Hawksworth, G.; Horne, V. A.; Newlands, A.; Morsman, J.; Tute, M. S.; Smith, D. A. Putative active site template model for cytochrome P4502C9 (tolbutamide hydroxylase). *Drug Metab. Dispos.* **1996**, *24*, 260–266.

(19) Ekins, S.; Bravi, G.; Binkley, S.; Gillespie, J. S.; Ring, B. J.; Wikel, J. H.; Wrighton, S. A. Three- and four-dimensional-quantitative structure activity relationship (3D/4D-QSAR) analyses of CYP2C9 inhibitors. *Drug Metab. Dispos.* **2000**, *28*, 994–1002.

(20) Rao, S.; Aoyama, R.; Schrag, M.; Trager, W. F.; Rettie, A.; Jones, J. P. A refined 3-dimensional QSAR of cytochrome P450 2C9: computational predictions of drug interactions. *J. Med. Chem.* **2000**, *43*, 2789–2796.

(21) PubChem Database. http://www.pubchem.org (accessed Oct 30, 2007).

(22) Heritage, T. W.; Lowis, D. R. Molecular Hologram QSAR. In *Rational Drug Design: Novel Methodology and Practical Applications*; American Chemical Society: Washington, DC, 1999; pp 212−225.

(23) Wendt, B.; Cramer, R. D. Quantitative series enrichment analysis (QSEA): a novel procedure for 3D-QSAR analysis. *J. Comput.-Aided Mol. Des.* **2008**, *22*, 541–551.

(24) Wendt, B.; Uhrig, U.; Bös, F. Capturing structure−activity-relationships from chemogenomic spaces. *J. Chem. Inf. Mod* **2011**, *51*, 843–851.

(25) Cramer, R. D. Topomer CoMFA: a design methodology for rapid lead optimization. *J. Med. Chem.* **2003**, *46*, 374–388.

(26) There is another plateau of LOO-q^2 values above 0.2 between training set sizes of 85−95 compounds (see Supporting Information p S10). No model was chosen from this plateau because of insufficient structural variation within the training set.

(27) Agarwal, A.; Pearson, P. P.; Taylor, E. W.; Li, H. B.; Dahlgren, T.; Herslöf, M.; Yang, Y.; Lambert, G.; Nelson, D. L.; Regan, J. W.; Martin, A. R. Three-dimensional quantitative structure−activity relationships of 5-HT receptor binding data for tetrahydropyridinylindole derivatives: a comparison of the Hansch and CoMFA methods. *J. Med. Chem.* **1993**, *36*, 4006–4014.

(28) Doweyko, A. M. 3D-QSAR illusions. *J. Comput.-Aided Mol. Des.* **2004**, *18*, 587–596.
(29) Golbraikh, A.; Tropsha, A. Beware of q^2!. *J. Mol. Graphics Modell.* **2002**, *20*, 269–276.
(30) Methoxy substituents represent potentially labile groups; however, in vivo studies later showed that introduction of the 4-methoxy group did not result in a metabolic liability for this series.